# Determination of the power transfer capacity of a UPFC with consideration of the system and equipment constraints and of installation locations

H. Cai, Z. Qu and D. Gan

**Abstract:** In this paper, power transfer capacity is investigated for systems with a unified power flow controller (UPFC). The combined effects of equipment constraints, system topology and installation locations on the UPFC real power transfer are studied. The P–Q characteristics of UPFC operation under different sets of constraints are determined. The admissible operational ranges of UPFC control outputs (in terms of the magnitude and phase angle of its series-injected voltage) are investigated, and the maximum power transfer and the maximum admissible range of power flow change are also found.

## 1 Introduction

The growth of electrical energy demand requires more transmission capacity, but the construction of new transmission facilities is constrained by environmental concerns and increasing costs. Flexible AC transmission system (FACTS) devices provide new alternatives in expanding the power transmission capacity of existing transmission lines. Several types of FACTS devices are available. The static VAr compensator (SVC) provides a direct and rapid bus voltage control that enhances power transmission, especially during low voltage conditions. The static synchronous compensator (STATCOM) [1] possesses the ability of providing faster response and greater reactive compensation than those from conventional synchronous condensers. The thyristor controlled series compensator (TCSC) can be used to change directly the power flow on a transmission line by controlling its impedance.

The unified power flow controller (UPFC) was developed based on a solid-state synchronous voltage source (STATCOM, SVS) [2, 3], and a phase-shifter [4]. It provides simultaneous, real-time control of all three power transmission parameters: voltage, impedance and phase angle. Therefore its deployment enables power system operators to better manage many transmission restrictions. For example, a UPFC device can handle such conventional functions as reactive shunt compensation, series compensation and phase shifting. More importantly, it can independently set and control the real and reactive power flow on a specific power transmission line, in order to maximise line utilisation and system capacity and/or to minimise reactive current flow (which in turn minimises power transmission losses) [5–7].



*IEE Proceedings* online no. 20020002

*DOI:* 10.1049/ip-gtd:20020002

Paper first received 24 July 2000 and in revised form 20 March 2001

H. Cai is with Invensys Process Automation (The Foxboro Company), 38 Neponset Ave., C42-2C, Foxboro, MA 02035, USA

Z. Qu is with the School of Electrical Engineering and Computer Science, University of Central Florida, Orlando, FL 32816, USA

D. Gan was with the School of Electrical Engineering and Computer Science, University of Central Florida, Orlando, FL 32816, USA

## 2 UPFC systems

Basically, a UPFC [5] consists of two voltage-sourced switching inverters, as shown by system 1 in Fig. 1. The series inverter is connected in series onto the transmission line, while the shunt inverter is linked to the terminal bus. The two inverters are interconnected via the DC link provided by a DC storage capacitor. The real power can flow in either direction between the two inverters, and each inverter can independently generate or absorb reactive power at its own AC terminals. The series inverter injects onto the line voltage an AC voltage $V_i \angle \theta_i$, whose magnitude and phase angle are controllable. Any real power exchange between the AC system and the series inverter is converted into DC power, and the amount of DC power is supplied or absorbed by the shunt inverter via the DC link. The shunt inverter can also be considered as a current source that provides independent reactive compensation for the transmission system, thus the shunt inverter can control the terminal voltage. The shunt current consists of two orthogonal elements: reactive current $I_q$ and active current $I_p$. It is current $I_p$ that balances the real power injected into the transmission line by the series inverter.

In this study, three systems with a UPFC will be considered. Parameters and operating conditions of the systems, shown in Fig. 1, are set to be:

*System 1*: $V_S = 1.015 \angle 10°$ p.u., $V_R = 1.0 \angle 0°$ p.u., and $Z_L = 0.01 + j0.1$ p.u.

*System 2*: $V_S = 1.03 \angle 30°$ p.u., $V_{R1} = 1.0 \angle 0°$ p.u., $V_{R2} = 1.02 \angle -5°$ p.u., $V_1 = 1.02$, $X_{s1} = 0.3$, $X_{s2} = 0.2$, $X_{L1} = 0.5$, $X_{L2} = 0.4$, $X_{12} = 0.25$

*System 3*: $V_{S1} = 1.03 \angle 30°$ p.u., $V_{S2} = 1.02 \angle 25°$ p.u., $V_{R1} = 1.0 \angle 0°$ p.u., $V_{R2} = 1.0 \angle 0°$ p.u., $V_1 = 1.02$, $V_2 = 1.015$, $X_{s1} = 0.2$, $X_{s2} = 0.15$, $X_{L1} = 0.4$, $X_{L2} = 0.2$, $X_{R1} = 0.3$, $X_{R2} = 0.25$, $P_{L1} = 0.1$, $P_{L2} = 0.4$

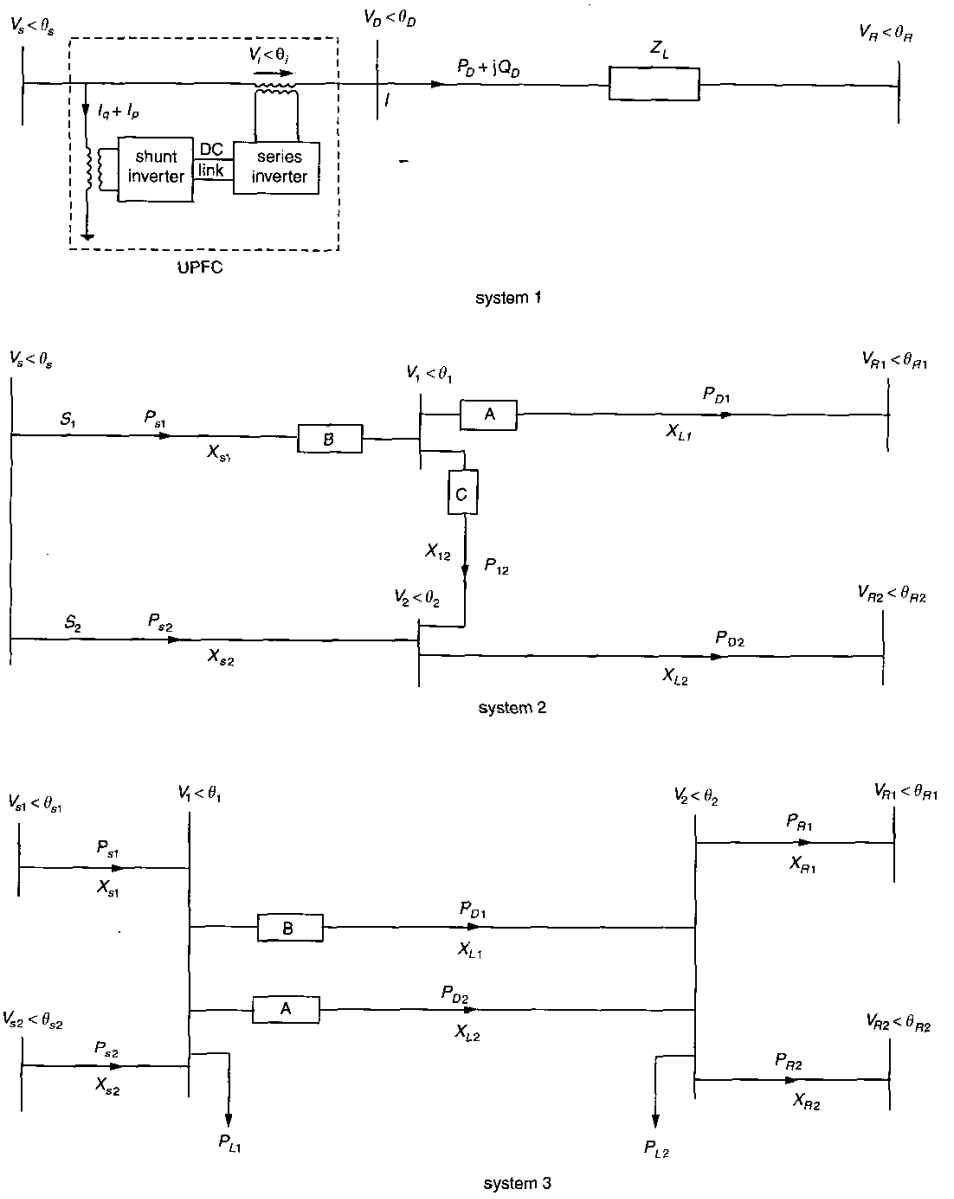


**Fig. 1** *Typical transmission systems with UPFC*

All the parameters above are given on a 100 MVA system base. To simplify power flow calculations for systems 2 and 3, it is assumed that the lines are lossless, that $V_2$ changes according to the resulting power flow, that the magnitude of $V_1$ is maintained by the UPFC, and that the voltages of the terminal buses at both sending and receiving sides are kept constant.

## 3 UPFC operation and control

The UPFC can be used to achieve all of the following objectives: terminal voltage regulation; series capacitive compensation; transmission angle regulation (phase shift) and combinations of the previous three. Superior to the conventional means, the most significant and powerful feature of the UPFC is its ability to control real and reactive power flow independently and in real-time.

Consider system 1 in Fig. 1. Quantities $V_S < \theta_S$ and $V_R < \theta_R$ are terminal voltages at the sending and receiving sides, respectively; $V_D < \theta_D$ is the line-side voltage; $Z_L$ denotes the line impedance; $I$ represents the line current; and $P_D + jQ_D$ is the power flow. The real and reactive power transfers are given by the following expressions:

$$\begin{aligned} P_D = \frac{1}{R^2 + X^2} \{ & (V_i \cos\theta_i + V_s \cos\theta_s) \\ & \times [(V_i \cos\theta_i + V_s \cos\theta_s - V_R \cos\theta_R) R \\ & + (V_i \sin\theta_i + V_s \sin\theta_s - V_R \sin\theta_R) X] \\ & + (V_i \sin\theta_i + V_s \sin\theta_s) \\ & \times [(V_i \sin\theta_i + V_s \sin\theta_s - V_R \sin\theta_R) R \\ & - (V_i \cos\theta_i + V_s \cos\theta_s - V_R \cos\theta_R) X] \} \end{aligned} \quad (1)$$

$$Q_D = \frac{1}{R^2 + X^2}\{-(V_i \cos\theta_i + V_s \cos\theta_s) \times [(V_i \sin\theta_i + V_s \sin\theta_s - V_R \cos\theta_R)R - (V_i \cos\theta_i + V_s \cos\theta_s - V_R \cos\theta_R)X] + (V_i \sin\theta_i + V_s \sin\theta_s) \times [(V_i \cos\theta_i + V_s \cos\theta_s - V_R \sin\theta_R)R + (V_i \sin\theta_i + V_s \sin\theta_s - V_R \sin\theta_R)X]\} \quad (2)$$

In eqns. 1 and 2, $P_D$ and $Q_D$ are expressed as functions of magnitude $V_i$ and phase angle $\theta_i$ of the injected voltage $V_i$. When there is no injected voltage, magnitude $V_i$ is 0 and the power flow is determined by the system's parameters and operating conditions. Given any voltage magnitude $V_i > 0$, the power flow solution varies in accordance with the change of phase angle $\theta_i$. By controlling both the magnitude $V_i$ and the phase angle $\theta_i$, a desired power transfer can always be reached before system and equipment constraints are taken into consideration. However, in reality, system and equipment constraints must be imposed, and the UPFC power transfer capacity must be determined accordingly.

## 4 UPFC power flow transfer capacity under system and equipment constraints

In this Section, the effects of the following system and equipment constraints on the UPFC power transfer capacity are studied one by one, in order to find both the admissible operational region of power transfer and the admissible ranges of the controllable parameters of the UPFC.

- magnitude of the series injected voltage: $0 \leq V_i \leq L_{V_i}$
- line current through the series inverter: $I \leq L_I$
- magnitude of the transmission-line side voltage: $L_{V_{D\min}} \leq V_D \leq L_{V_{D\max}}$
- real power exchange between the series inverter and shunt inverters: $|P_{DC}| \leq L_{P_{DC}}$
- shunt inverter current: $I_{sh} \leq L_{I_{sh}}$

Bounds $L_{V_i}, L_I, L_{V_{D\max}}, L_{V_{D\min}}, L_{P_{DC}}$ and $L_{I_{sh}}$ are self explanatory and $I_{sh} = \sqrt{I_q^2 + I_p^2}$.

### 4.1 Injected voltage constraint $0 \leq V_i \leq L_{V_i}$

It follows from eqns. 1 and 2 that, given the series injected voltage $V_i$, $P_D$ and $Q_D$ are functions of the phase angle $\theta_i \in [0°, 360°]$ from which a set of level curves in the P–Q plane can be solved, as shown in Fig. 2. In this Figure, for a given value of $L_{V_i}$, the level curve is an ellipse, and its interior represents all the possible values of $P_D$ and $Q_D$ for $0 \leq V_i \leq L_{V_i}$ and $0° \leq \theta_i \leq 360°$. The smaller the value $L_{V_i}$, the smaller the ellipse and the region of power transfer. In other words, to obtain the maximum power transfer capacity, $V_i$ should be set to its upper bound $L_{V_i}$ (if no other constraints are imposed).

### 4.2 Line current constraint $I \leq L_I$

The line current through the series inverter $I$ can be calculated by

$$I = (V_S + V_i - V_R)/Z_L \quad (3)$$

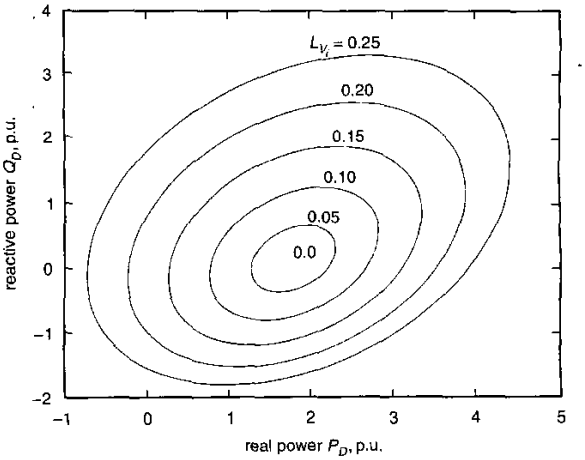


**Fig. 2** *P–Q characteristics under a set of bounds of the voltage $V_i$*

The current bound $L_I$, in the form of $I \leq L_I$, can be rewritten as

$$\cos(\theta_i - \varphi_{Z_L} - \varphi_{I_0}) \leq \frac{Z_L}{2I_0V_i}\left(L_I^2 - I_0^2 - \frac{V_i^2}{Z^2}\right) \quad (4)$$

where $\varphi_{Z_L}$ and $\varphi_{I_0}$ are phase angles of $Z_L(= R + jX)$ and $I_0(= (V_S - V_R)/Z_L)$, respectively; and $Z_L$, $V_S$ and $V_R$ are those defined previously.

The P–Q level curves and the corresponding boundaries for $L_I = 4.15$ p.u. and $L_I = 3.5$ p.u. with $L_{V_i} = 0.25$ p.u. are the dash lines in Fig. 3. The solid line in Fig. 3 represents the P–Q characteristics with $V_i = L_{V_i} = 0.25$ p.u. Therefore the admissible power transfer under a given current bound $L_I$ is the region that is the subset of the ellipse and to the left of the corresponding dash line. From the Figure, it is straightforward to see that introducing a line current bound reduces the maximum real power transfer of the UPFC obtained only under the voltage bound $L_{V_i}$.

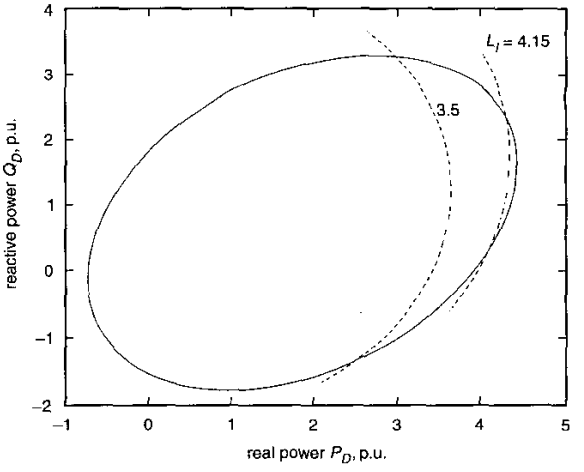


**Fig. 3** *P–Q characteristics with the line current bounds $L_I$=4.15 p.u. and $L_I$=3.5 p.u.*

### 4.3 Line voltage constraint $L_{V_{D\min}} \leq V_D \leq L_{V_{D\max}}$

The transmission line voltage of the UPFC (at its output side) can be calculated by

$$V_D = V_i - V_R \quad (5)$$

Therefore constraint $L_{V_{D\min}} \leq V_D \leq L_{V_{D\max}}$ can be imposed through the following two inequalities on the $V_i - \theta_i$ relations:

$$\cos(\theta_i - \theta_S) \leq \frac{1}{2V_iV_S}(L^2_{V_{D\max}} - V_i^2 - V_S^2) \quad (6)$$

$$\cos(\theta_i - \theta_S) \geq \frac{1}{2V_iV_S}(L^2_{V_{D\min}} - V_i^2 - V_S^2) \quad (7)$$

Mapped into the P–Q plane using eqns. 1 and 2, this constraint (with $L_{V_i} = 0.25$ p.u., $L_{V_{D\min}} = 0.9$ p.u., and $L_{V_{D\max}} = 1.1$ p.u.) is shown in Fig. 4. It is obvious from Fig. 4 that this constraint does not have much impact on the maximum real power transfer, but it noticeably restricts the admissible ranges of $Q_D$ and the phase angle $\theta_i$.

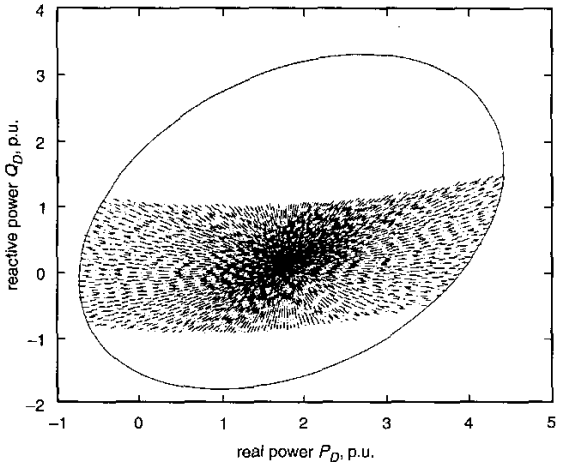


**Fig. 4** *P–Q characteristics with 0.9 p.u. ≤ $V_D$ ≤ 1.1 p.u. and $L_{V_i}$ = 0.25 p.u.*

### 4.4 DC power constraint $|P_{DC}| \leq L_{P_{DC}}$

Real power exchange capacity between the series inverter and the shunt inverter is limited by the UPFC DC link configuration. Constraint $|P_{DC}| \leq L_{P_{DC}}$ is equivalent to the inequalities:

$$\sin(\theta_i + \alpha) \leq \frac{1}{V_i\sqrt{E^2 + F^2}}(L_{P_{DC}}(R^2 + X^2) - RV_i^2) \quad (8)$$

and

$$\sin(\theta_i + \alpha) \geq \frac{1}{V_i\sqrt{E^2 + F^2}}(-L_{P_{DC}}(R^2 + X^2) - RV_i^2) \quad (9)$$

where $\alpha = \sin^{-1}(E/\sqrt{E^2 + F^2})$, $E = RV_S\cos\theta_S - RV_R\cos\theta_R + XV_S\sin\theta_S - XV_R\sin\theta_R$ and $F = RV_S\sin\theta_S - RV_R\sin\theta_R - XV_S\cos\theta_S + XV_R\cos\theta_R$. The region for admissible power transfers $P$ and $Q$ can be easily drawn, and its shape is similar to that in Fig. 4. One interesting phenomenon revealed from such a region is that the constraint on the DC link real power exchange has no direct impact on the real power transfer of the UPFC. It affects the reactive power transfer capacity of the UPFC and it restricts the range of the phase angle $\theta_i$. This indicates that most of the real power transfer controlled by the UPFC does not flow through the DC link between the two inverters of the UPFC.

### 4.5 Shunt current constraint $I_{sh} \leq L_{I_{sh}}$

The shunt inverter current $I_{sh}$ is the magnitude of two elements: reactive current $I_q$ and active current $I_p$. Current $I_q$ is independently controlled by the UPFC so as to provide shunt reactive compensation, and its change, in turn, controls the terminal voltage. The upper bound on $I_q$ is determined by the UPFC shunt reactive compensation rating. Since $I_p$ is to balance the real power injected into the line by the UPFC series inverter and hence must be in phase with the input terminal voltage, it can be calculated by

$$I_p = P_{DC}/V_S \quad (10)$$

where $P_{DC} = \mathrm{Re}(V_iI^*)$. Thus, it follows that

$$I_{sh} = \sqrt{I_q^2 + (P_{DC}/V_S)^2} \quad (11)$$

Note that $P_{DC}$ is usually smaller than 1, and the term $(P_{DC}/V_S)^2$ in eqn. 11 is relatively small. Thus, bound $L_{I_{sh}}$ will mainly restrict the shunt reactive compensation of the UPFC. In other words, bound $L_{I_{sh}}$ will not much affect the power transfer capacity, as long as the shunt inverter reactive compensation rating is designed to be large enough.

### 4.6 Power transfer capacity and available ranges of UPFC control parameters under constraints

For implementation, the UPFC power transfer capacity needs to be found when all the constraints discussed previously are imposed together. The un-shaded region inside the ellipse in Fig. 5 is the admissible power transfer region. Roughly, $P_D$ can change between −0.8 p.u. to 3.7 p.u., and $Q_D$ can vary between −1.0 p.u. and 1.0 p.u. Corresponding to the P–Q characteristics shown in Fig. 5, ranges of the UPFC control parameters (magnitude and phase angle of the series injected voltage) are plotted as the un-shaded area in Fig. 6. As long as $V_i$ and $\theta_i$ are chosen within this region, the UPFC operates without violating any of the aforementioned system and equipment constraints.

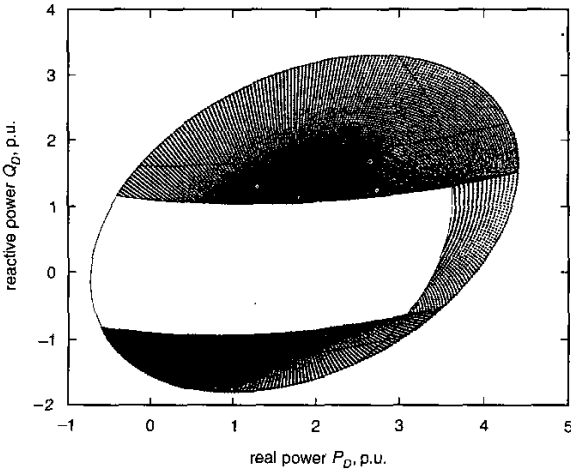


**Fig. 5** *P–Q characteristics under all the constraints*

For any pair of values of $V_i$ and $\theta_i$ in the un-shaded region of Fig. 6, one can calculate the real power transfer $P_D$. The relationship between the maximum real power transfer $P_D$ and $V_i$ is given by Fig. 7, and the relationship between the maximum real power transfer $P_D$ and $\theta_i$ is shown in Fig. 8. Note that Fig. 7 is obtained by fixing the value of $V_i$, while maximising $P_D$ with respect to $\theta_i$.

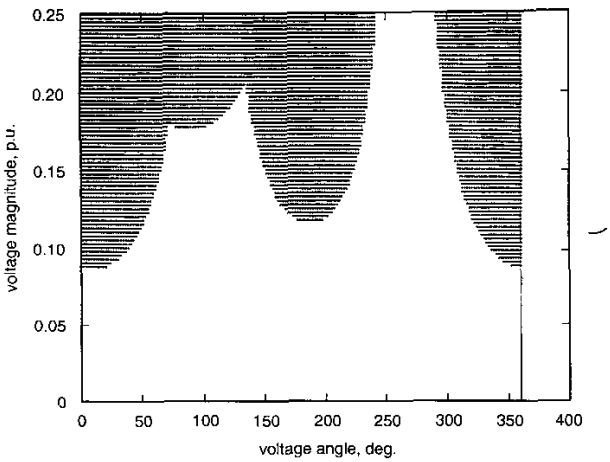


**Fig. 6** *Admissible values of $V_i$ and $\theta_i$ under constraints*

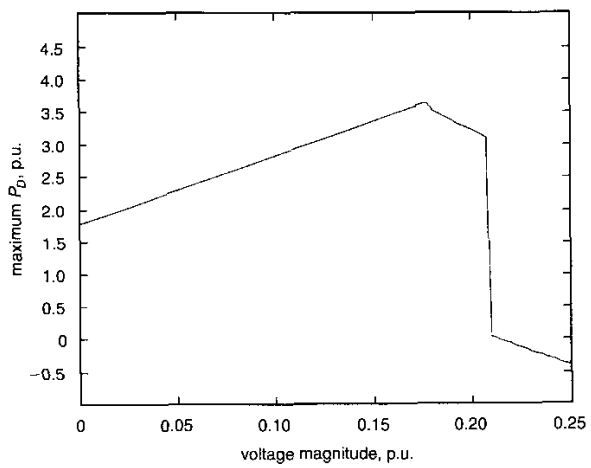


**Fig. 7** *Maximum real power transfer versus $V_i$, maximised with respect to $\theta_i$*

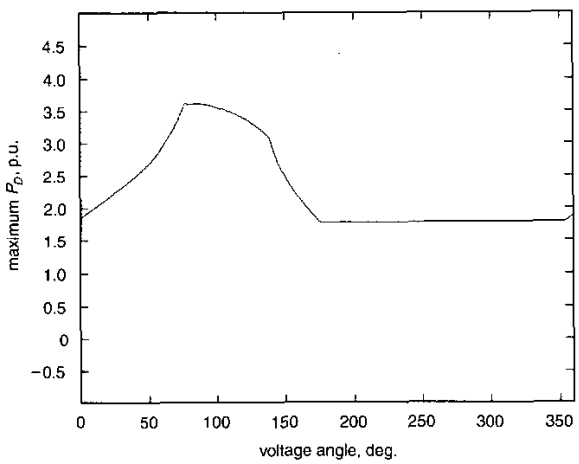


**Fig. 8** *Maximum real power transfer versus $\theta_i$, maximised with respect to $V_i$*

Similarly, Fig. 8 is drawn by fixing the value of $\theta_i$, while maximising $P_D$ with respect to $V_i$. Figs. 7 and 8 combined can be used to choose the UPFC operating point that would achieve the maximum real power transfer. An important conclusion that can be reached from Fig. 7 is that the maximum real power transfer is not obtained at the upper bound of $V_i$. This is different from the conclusion made in Section 4.1, where no constraint other than upper bound $L_{V_i}$ is imposed. Therefore, to achieve the maximum real power transfer, the magnitude and phase angle should be chosen together, taking into consideration all the constraints.

In most cases, power flow control should give, not only high-level real power transfer but also, an adequate range of admissible power changes (thus the flexibility of UPFC control). The relationship of the phase angle $\theta_i$ to the real power transfer $P_D$ is shown in Fig. 9 for a set of values of $V_i$. Although a larger amount of real power transfer can be achieved when $V_i$ is chosen to be between 0.15 p.u. and 0.175 p.u., the phase angle $\theta_i$ is limited within a small range, and so is the admissible range of real power transfer. To have a relatively large continuous range for real power adjustment and the largest continuous operational range of the phase angle $\theta_i$, the magnitude $V_i$ should be chosen to be around 0.1 p.u. Therefore, a tradeoff should be made to determine the UPFC operational mode, since both features (larger maximum real power transfer and an adequate range of real power control) are important for power-system steady-state security and dynamic security.

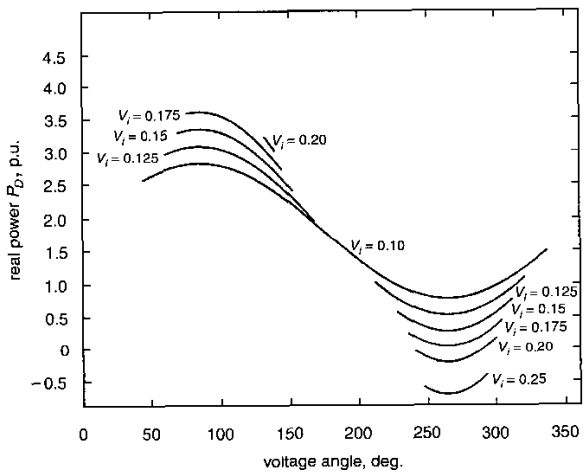


**Fig. 9** *Real power transfer $P_D$ against phase angle $\theta_i$ for a set of magnitude $V_i$*

## 5 Power transfer capacity against system structure and UPFC locations

The constraints discussed in the previous Sections come from equipment considerations and the steady-state security of the transmission line. Besides these constraints, the power transfer capacity of a UPFC-equipped system will also be limited by its transmission system structure and its location. To study the impact of the system structure and the UPFC location, systems 2 and 3 in Fig. 1 are investigated here.

We begin with system 2. If the UPFC is at location A, the UPFC can increase the real power transfer setting $P_{D1}$, in which case more power is drawn from the sending side via lines $S_1$ and $S_2$, and the total power transfer $P_{D1} + P_{D2}$ is increased. However, this does not mean $P_{D2}$ will be increased. As shown in Fig. 10, this is due to the fact that $P_{12}$ changes its direction as $V_1$ and $V_2$ change.

If the UPFC is located on line $S_1$ and at location B, the UPFC can increase $P_{s1}$, but $P_{s2}$ eventually flows back to

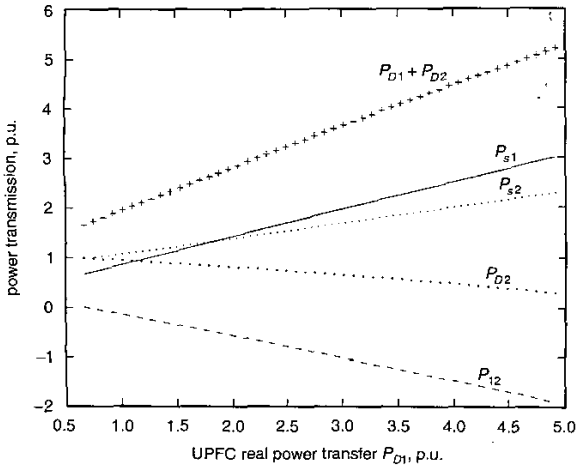


**Fig. 10** *Real power transfer on system 2 with the UPFC at location A*

the sending side through line $S_2$ as the UPFC real power transfer setting increases. As shown in Fig. 11, the maximum total power transfer (about 3.6 p.u.) is reached when the UPFC real power setting is chosen to be 4.4 p.u. In this case, about 0.8 p.u. real power goes back to the sending side through line $S_2$. The existence of this upper limit (the maximum total power transfer) is due to the nature of the system power flow distribution. Therefore, the maximum power transfer value depends upon the system parameters, especially line impedance and the operation conditions. Compared to the case that UPFC is at location B, the total real power transfer with the UPFC at location A is about 5.0 p.u. with the same UPFC real power setting (4.4 p.u.), and the former is 1.4 p.u. (5.0−3.6) higher.

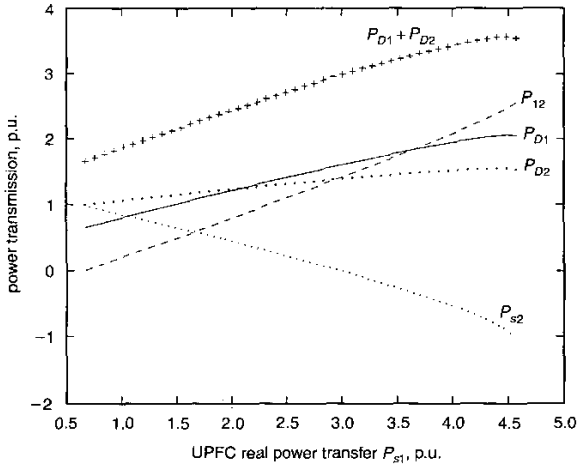


**Fig. 11** *Real power transfer on system 2 with the UPFC at location B*

For the purpose of increasing the total real power transfer, location C is not a good place to install the UPFC. This conclusion is quite intuitive, and it is verified by the result in Fig. 12. Although a new maximum value of the total real power transfer can be found by changing the UPFC real power setting, this maximum value does not have any practical significance. More importantly, the change of power flow in either direction does not really change much the total power transfer. More very clear evidence one can observe from Fig. 12 is that power flows change significantly with respect to the change of the UPFC setting.

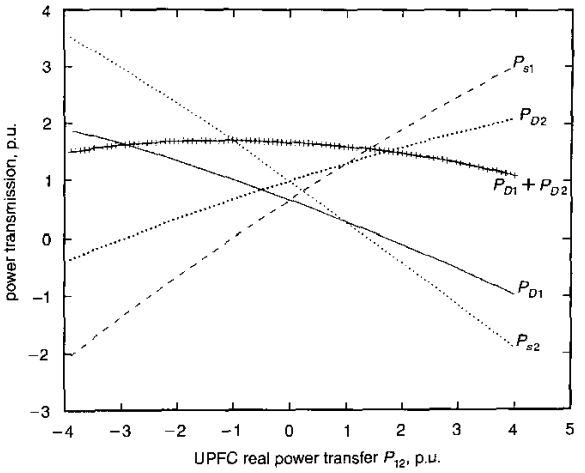


**Fig. 12** *Real power transfer on system 2 with the UPFC at location C*

A comparison of the total real power transfer capacity of system 2 among these possible locations of the UPFC is given in Fig. 13. It is obvious that, given the same setting of the UPFC, location A provides the largest total real power transfer.

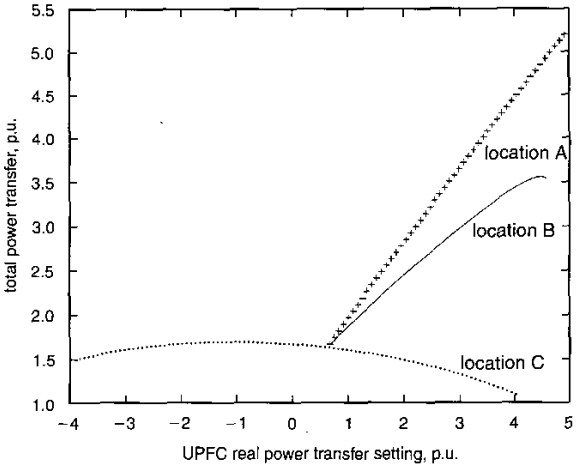


**Fig. 13** *Total real power transfer of system 2 with the UPFC at location A or B or C*

Similar calculations can be carried out for system 3 with respect to locations A and B for the UPFC. The initial power flows on the parallel lines are $P_{D1} = 1.0$ p.u. and $P_{D2} = 0.5$ p.u., and the difference is due to line impedances. Fig. 14 show the power flow and total real power transfer under a set of UPFC real power settings for the UPFC to be at locations A and B, respectively. It is clear that, if the UPFC setting is chosen higher than a certain value (about 2.4 p.u. for both locations), the real power begins to flow back to one of the sources through the other parallel line. Another observation is that more power transfer can be

achieved when the UPFC is installed on line 2 that has a smaller initial power flow (due to the larger value of its line impedance).

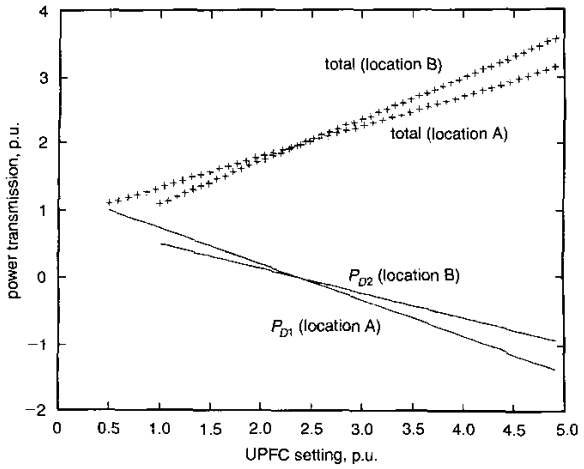


**Fig. 14** *Real power transfer of system 3 with the UPFC at locations A and B*

## 6 Conclusions

A UPFC can effectively increase real power transfer, and several constraints on the system and equipment must be taken into account in determining the rating, siting and operation mode of a UPFC.

Admissible operation ranges of the UPFC series injected voltage have been found, and the maximum value of the power transfer has been calculated for the case that the voltages of the terminal buses on both sides of the transmission line are fixed. A tradeoff between the operational range of the UPFC control (magnitude and phase angle of the series injected voltage) and the maximum power transfer should be made to yield a significant (less than the maximum) real power transfer and an adequate, continuous range of real power control.

In order to increase the total real power transfer, a UPFC is better located on the transmission line directly connected to the receiving side of the system. The increase of the UPFC real power transfer setting may result in a portion of the power flowing back to one of the power sources through the other transmission lines, when parallel transmission lines are present. In a system with parallel transmission lines at the local side, the UPFC is better located on the line with higher line impedance (which results in smaller initial power flow), regardless of line losses. Such an installation will increase the total power transfer.

## 7 References


1 LARSEN, E., MILLER, N., NILSSON, S., and LINDGREN, S.: 'Benefits of GTO-based compensation systems for electric utility applications', *IEEE Trans. Power Deliv.*, 1992, **7**, (4), pp. 2056–2062
2 GYUGYI, L.: 'Dynamic compensation of ac transmission lines by solid-state synchronous voltage sources', *IEEE Trans. Power Deliv.*, 1994, **9**, (2), pp. 904–911
3 HATZIADONIU, C.J., and FUNK, A.T.: 'Development of a control scheme for a series-controlled solid-state synchronous voltage source', *IEEE Trans. Power Deliv.*, 1966, **11**, (2), pp. 1138–1143
4 OOI, B., DAI, S., and GALIANA, F.: 'A solid-state pwm phase-shifter', *IEEE Trans. Power Deliv.*, 1993, **8**, (2), pp. 573–579
5 GYUGYI, L., RIETMAN, T.R., and EDRIS, A.: 'The unified power flow controller: a new approach to power transmission control', *IEEE Trans. Power Deliv.*, 1995, **10**, (2), pp. 1085–1093
6 NELSON, R.J., BIAN, J., and WILLIAMS, S.L.: 'Transmission series power control', *IEEE Trans. Power Deliv.*, 1995, **10**, (1), pp. 504–510
7 BIAN, J., RAMEY, D.G., NELSON, R.J., and EDRIS, A.: 'A study of equipment sizes and constraints for a unified power flow controller', *Proceedings of the IEEE Transmission and Distribution Conference*, 1996, Los Angeles, CA, pp. 332–338